Proceedings of ALGORITMY 2000
Conference on Scientific Computing, pp. 28–36

NUMERICAL SIMULATIONS OF RADIONUCLIDES TRANSPORT IN DOUBLE POROSITY MEDIA WITH SORPTION *

PETER FROLKOVIČ † AND JÜRGEN GEISER ‡

Abstract. A mathematical model of the transport of radionuclides in double porosity media with sorption processes is presented. A comparison of numerical solutions with a semi-analytical solution for a simplified example is described.

Key words. radionuclide transport, sorption, double porosity, numerical simulations

AMS subject classifications. 76S05, 80A32, 65M60

1. Introduction. A safety study of radioactive waste disposals requires mathematical modelling of risk scenarios where several different physical processes are considered. Such a model should not restrict only to the description of the advective-dispersive multicomponent transport in porous media with decay chain of radionuclides, but it should include the modelling of the exchange processes between the mobile and the "immobile" pore groundwater and the kinetic sorption processes [5, 7].

In the next section such a mathematical model will be described. The description is based on a mass balance formulation and in such a way it is "ready-to-use" for the numerical discretization by finite volume methods. The used numerical methods are briefly described in the section 3. The numerical results for a test example where semi-analytic solution is known, are presented in the last section together with a brief discussion of a more complex test example.

2. Mathematical model. We supposed that the volume V of porous media can be divided into 4 parts - the first two subvolumes that are occupied by a "mobile" (flowing) pore groundwater and an "immobile" (steady) pore groundwater and the second pair of subvolumes that represents the solid matrix of aquifer.

Each solute of the next described multicomponent system can occur in each part of the porous media. In such a way the concentration C^i of the i-th solute can be considered as the sum of 4 corresponding *unknown* concentrations - C_L^i (the concentration in the mobile groundwater [mol/m^3]), G_L^i (the concentration in the immobile groundwater [mol/m^3]), C_{Ad}^i (the concentration of the adsorbed solute from the mobile groundwater [mol/kg]) and G_{Ad}^I (the concentration of the adsorbed solute from the immobile groundwater [mol/kg]).

The mass of the i-th solute in V can be determined then from

$$\int_V C^i dx = \int_V \phi C_L^i dx + \int_V \phi_{im} G_L^i dx +$$

$$\int_V g(1-\phi-\phi_{im})\rho C_{Ad}^i dx + \int_V (1-g)(1-\phi-\phi_{im})\rho G_{Ad}^i dx\,.$$

* This work was (partially) funded by the German Federal Ministry of Economics and Technology (BMWi) under the contract No 02 E 9148 2

†Peter.Frolkovic@IWR.Uni-Heidelberg.DE

‡Juergen.Geiser@IWR.Uni-Heidelberg.DE, Technische Simulationen IWR, Im Neuenheimer Feld 368, 69120 Heidelberg, Germany

In above ϕ and ϕ_{im} denote the corresponding porosities of the volume V that characterize the parts occupied by the mobile and the immobile water. Moreover, the factor $g \in (0,1)$ divides the solid matrix part of V (characterized by the porosity $(1-\phi-\phi_{im})$) between two parts where the adsorbed solute of the concentration C^i_{Ad}, respectively G^i_{Ad}, occurs. Finally, ρ [kg/m^3] denotes the density of solid matrix.

Further, we consider a first order decay chain of nuclides with λ^i denoting the decay constant rate of the i-th nuclide and $k = k(i)$ denotes the index of the produced nuclide. Following [5] we consider the same decay constants in each of 4 parts of porous media.

Next we describe the partial differential equations for the unknowns C^i_L, G^i_L, C^i_{Ad} and G^i_{Ad}. If so called "equilibrium" (fast) sorption occurs, the system is reduced for the unknowns C^i_L and G^i_L only, see a description later.

2.1. Mobile pore groundwater. Following [5] one has to consider that each i-th nuclide belongs to an "element" e, i.e. $e = e(i)$. Moreover, some parameters can depend on the concentration $C^{e(i)}_L$ of the element e that is given by

$$C^{e(i)}_L := \sum_i C^i_L \tag{2.1}$$

and where i runs through the indices of all nuclides that belongs to the element e.

The transport of the solute in the mobile groundwater that includes the sinks and the sources due to the decay chain and due to the exchange processes with other parts of the porous media, can be described by [7, 5]

$$\phi\left(\partial_t C^i_L + \lambda^i C^i_L - \sum_{k=k(i)} \lambda^k C^k_L\right) + \nabla\cdot(\vec{q}C^i_L - D\nabla C^i_L) + \tag{2.2}$$

$$\alpha^{e(i)}(C^i_L - G^i_L) + k^{e(i)}(K(C^{e(i)}_L)C^i_L - C^i_{Ad}) = 0\,.$$

In (2.2) by $\vec{q}$ we denote the velocity field that fulfills $\nabla\cdot\vec{q} = 0$. Further, D denotes the diffusive-dispersive tensor [3]

$$D := \phi d^{e(i)}T + |\vec{q}|(\alpha_T + (\alpha_L - \alpha_T)\vec{q}^T\cdot\vec{q}/|\vec{q}|^2)$$

where $d = d^e$ denotes the molecular diffusion for the e-th element, T denotes the tortuosity tensor and finally α_T and α_L denote the transversal, respectively the longitudinal dispersions.

The rate constants $\alpha^{e(i)}$ characterize the exchange of the e-th solute element between the mobile and the immobile groundwater and $k^{e(i)}$ characterize the rate constants of the sorption kinetic.

The particular form of the coefficient $K = K(C^{e(i)}_L)$ depends on the type of the used sorption isotherm. For the simplest linear case (Henry isotherm) K is a constant, the nonlinear cases of Freundlich isotherm [5]

$$K = K(C^{e(i)}_L) = K_{nl}\left(C^{e(i)}_L\right)^{p-1} \tag{2.3}$$

and/or Langmuir isotherm [5]

$$K = K(C^{e(i)}_L) = \frac{\kappa b}{1 + bC^{e(i)}_L} \tag{2.4}$$

are also considered.

2.2. Immobile pore groundwater.

$$\phi_{im}\left(\frac{\partial}{\partial t}G_L^i + \lambda^i G_L^i - \sum_{k=k(i)}\lambda^k G_L^k\right) + \tag{2.5}$$

$$+\,\alpha^{e(i)}(G_L^i - C_L^i) + k^{e(i)}(K(G_L^{e(i)})G_L^i - G_{Ad}^i) = 0\,.$$

Here, an analogous description as in the previous subsection could be used, except that no convection, diffusion and dispersion transport is considered here. The concentration $G_L^{e(i)}$ is defined analogously to (2.1).

2.3. Adsorption from the mobile groundwater.

$$g(1-\phi-\phi_{im})\rho\left(\frac{\partial}{\partial t}C_{Ad}^i + \lambda^i C_{Ad}^i - \sum_{k=k(i)}\lambda^k C_{Ad}^k\right) = \tag{2.6}$$

$$k^{e(i)}\left(K(C_L^{e(i)})C_L^i - C_{Ad}^i\right)\,.$$

The right hand side of (2.6) occurs as the last term in (2.2). If it is replaced there by the left hand side of (2.6) then one has the equivalent form of (2.2)

$$\phi\left(\frac{\partial}{\partial t}C_L^i + \lambda^i C_L^i - \sum_{k=k(i)}\lambda^k C_L^k\right) + \tag{2.7}$$

$$g(1-\phi-\phi_{im})\rho\left(\frac{\partial}{\partial t}C_{Ad}^i + \lambda^i C_{Ad}^i - \sum_{k=k(i)}\lambda^k C_{Ad}^k\right) +$$

$$\nabla\cdot(\vec{q}C_L^i - D\nabla C_L^i) + \alpha^{e(i)}(C_L^i - G_L^i) = 0\,.$$

Moreover, if the fast sorption is considered (i.e. $1/k^{e(i)} \to 0$ in (2.6)) then C_{Ad}^i is given explicitly by

$$C_{Ad}^i = K(C_L^{e(i)})C_L^i \tag{2.8}$$

and only the equation (2.7) for C_L^i is considered instead of (2.2) and (2.6).

2.4. Adsorption from the immobile groundwater.

$$(1-g)(1-\phi-\phi_{im})\rho\left(\frac{\partial}{\partial t}G_{Ad}^i + \lambda^i G_{Ad}^i - \sum_{k=k(i)}\lambda^k G_{Ad}^k\right) =$$

$$k^{e(i)}\left(K(G_L^{e(i)})G_L^i - G_{Ad}^i\right)\,. \tag{2.9}$$

Analogous description as in the subsection 2.3 can be used here.

3. Numerical methods. The system (2.2), (2.5), (2.6) and (2.9) is discretized using the so called "vertex-centred" finite volume method. The basic idea behind this method is a construction of a dual mesh of finite volumes (FV) that is complementary to a standard finite element (FE) mesh. The unknown discrete variables are placed in the vertices of the triangulation and for each vertex x_j a finite volume V_j is constructed.

The unknown numerical solution is constructed using well-known conforming FE test functions and the discrete equations are constructed using local mass balance formulation on the dual mesh. Such methods are very often called the "control volume FE" [10] or the "FV element methods" [4].

A package RNT (Radio-Nuclides Transport) for the numerical solution of (2.2) - (2.9) is developed using the powerful numerical library UG (Unstructured Grid) [1]. It is based on the implementation of the multicomponent reactive transport using an effective memory format for the sparse matrices [8]. The future development should include a coupling with the so called "density driven flow" where the velocity field $\vec{q}$ fulfills more complex non-stationary flow equation [6].

If one of nonlinear form of the sorption isotherms is used (2.3) - (2.4) then the resulting algebraic system will be solved by Newton method with an analytical linearization. The resulting linear algebraic systems are solved by a biconjugate gradient method with a multigrid linear solver as a preconditioner. The time discretization is the implicit Euler method.

4. Numerical results. For a linear case of the system (2.2) - (2.9) and for a simple form of $\vec{q}$ special analytical solutions can be found [7, 2]. They describe typically a time evolution of the concentration from a singular point source.

To validate the developed software package RNT the example of 4 species transport with the retardation (fast sorption) and without immobile groundwater (i.e. $\alpha^{e(i)} \equiv 0$) was computed and the results were compared with the corresponding semi-analytical solution. In a near future a comparison with semi-analytical solutions for non-simplified system (2.2) - (2.9) should be provided.

The particular form of the equation (2.7) for $i = 1, 2, 3, 4$ is given then by

$$R^i \partial_t C_L^i + R^i \lambda^i C_L^i - R^{i-1} \lambda^{i-1} C_L^{i-1} + \nabla \cdot (\vec{q} C_L^i - D \nabla C_L^i) = 0 \tag{4.1}$$

where $\lambda^0 \equiv 0$. The decay constants correspond to the decay of chemical species Perchlorethen, Trichlorethen, Dichlorethen and Vinylchlorid and they take the values $\lambda^1 = 7.6$, $\lambda^2 = 2.2$, $\lambda^3 = 2.1$ and $\lambda^4 = 2.0$ [10^{-4} 1/d]. The velocity field takes the constant value $\vec{q} = (0.2, 0.0)$ [m/d]. The molecular diffusion is neglected by taking $d^i \equiv 0$ and the dispersion constants are taken to be $\alpha_L = 6.8$ and $\alpha_T = 0.2$ [m]. The retardation factors are given by $R^1 = 8.0$, $R^2 = 2.0$, $R^3 = 1.1$ and $R^4 = 1.0$.

The above problem is analytically studied for the case of unbounded domain in R^2 and for nonzero initial conditions for C_L^1 only consisting of a singular "point impulse" $C_{const}^1 \delta(x, y)\delta(t)$ with δ being a well-known delta function. The analytical solution can be described explicitly for C_L^1, to compute other components C_L^2, C_L^3 and C_L^4 the so called "Hantush function"

$$W(a_1, a_2) = \int_{a_1}^{\infty} \frac{1}{\xi} \exp\left(-\xi - \frac{a_2^2}{4\xi}\right) d\xi \tag{4.2}$$

must be evaluated numerically [7]. The complexity of the analytical solution grows from the definition of C_L^2 to C_L^4. To evaluate $C_L^2(x, t)$ the function W has to be

computed for two values of (a_1, a_2), to evaluate $C_L^4(x,t)$ once the function W has to be computed for 24 different values of (a_1, a_2). The integral in (4.2) was computed numerically by using the Gaussian quadrature with 10 integration points per each subinterval [9].

To avoid numerical difficulties by approximating the singular form of the solution at $t = 0$ and $(x, y) = (0, 0)$, the values of the analytical solution at $t = 100$ were taken as the initial conditions. The domain was taken to be a rectangle with the left bottom corner $(-500, -100)$ and the right top corner $(1300, 100)$. The boundary conditions were zero flux B.C. at the top and the bottom of the domain and the inflow B.C. with $C_L^i = 0$ on the left and the outflow B.C. at the right part of the rectangle. The initial conditions for the numerical solution and the results at $t = 2000$ days are presented in the Figure 4.1.

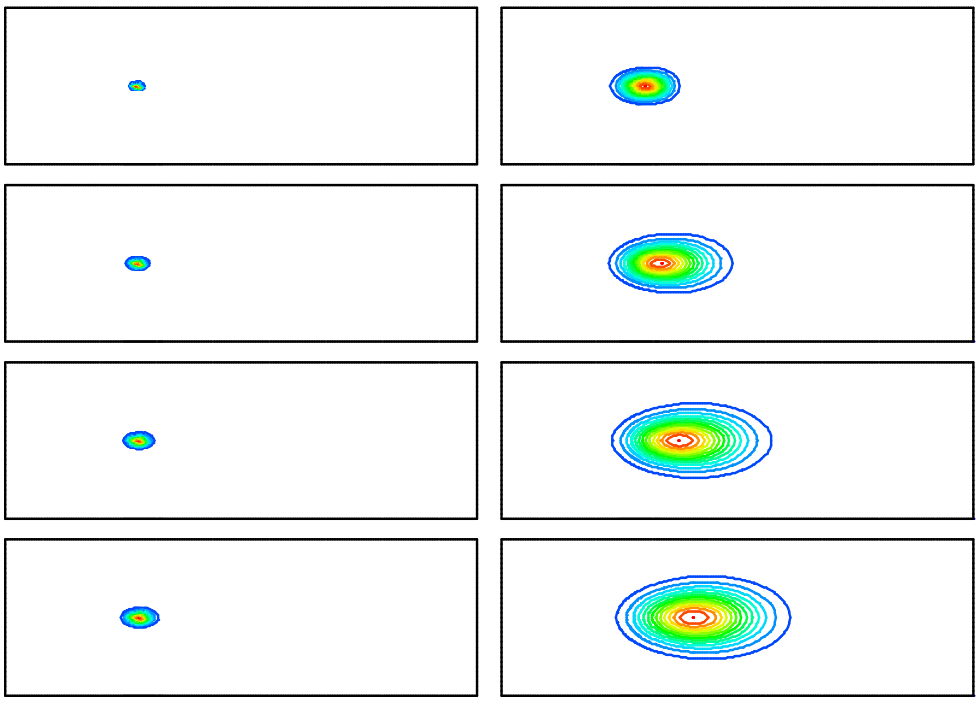

FIG. 4.1. C_L^i *for* $i = 1, ..., 4$ *at* $t = 100$ *days (initial conditions) and* $t = 2000$ *days.*

The pictures were stretched in y direction. The contour lines are plotted from the corresponding minimal value to the maximal value of the particular component of the numerical solution. The initial grid, consisting of 6 square elements, was refined using a combination of a uniform refinement and a local refinement around the point $(0, 0)$ with the grid step h varying from $h = 200/(2^5)$ to $h = 200/(2^{10})$ [m]. The final grid consists of 7690 elements. The time step was chosen $\tau = 1$ day.

The relative discrete maximum error for each time was computed by

$$u_N^{rel}(t_m) := \frac{\max_{j=1,...,N} |u_N(x_j, t_m) - u_{exact}(x_j, t_m)|}{\max_{j=1,...,N} |u_{exact}(x_j, t_m)|}$$

where N is the number of vertices for a particular grid. The values of this error for each component C_L^i at each discrete time are plotted in the Figure 4.2.

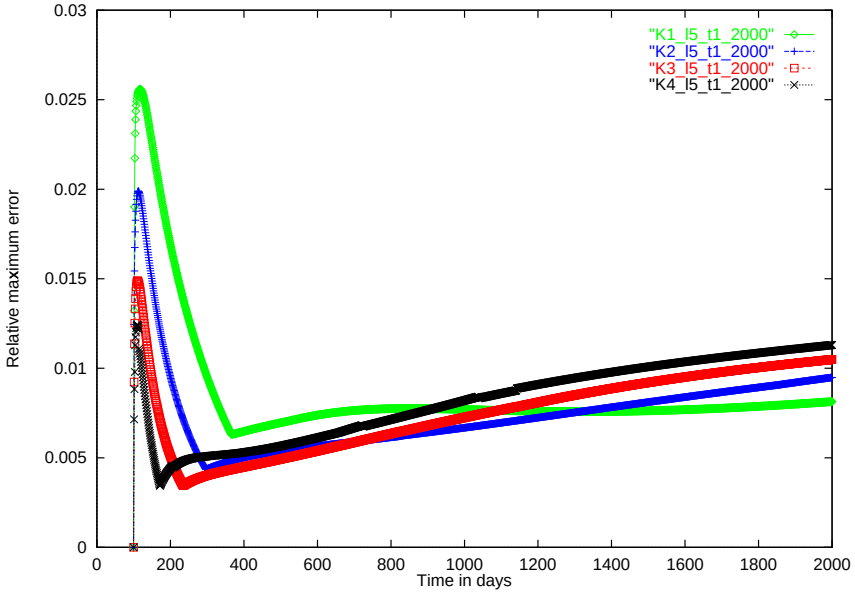

FIG. 4.2. *The relative maximum error for 4 components of the numerical solution*

To illustrate the convergence of the numerical solution we compare the error for 2 successive grids. In the Figure 4.3 the error for the numerical solution from the Figure 4.2 is compared with the one on a finer grid (once more uniformly refined with 22 056 elements) with the identical fixed time step $\tau = 1$ day. It is clear that the grid refinement decreases significantly further the numerical error.

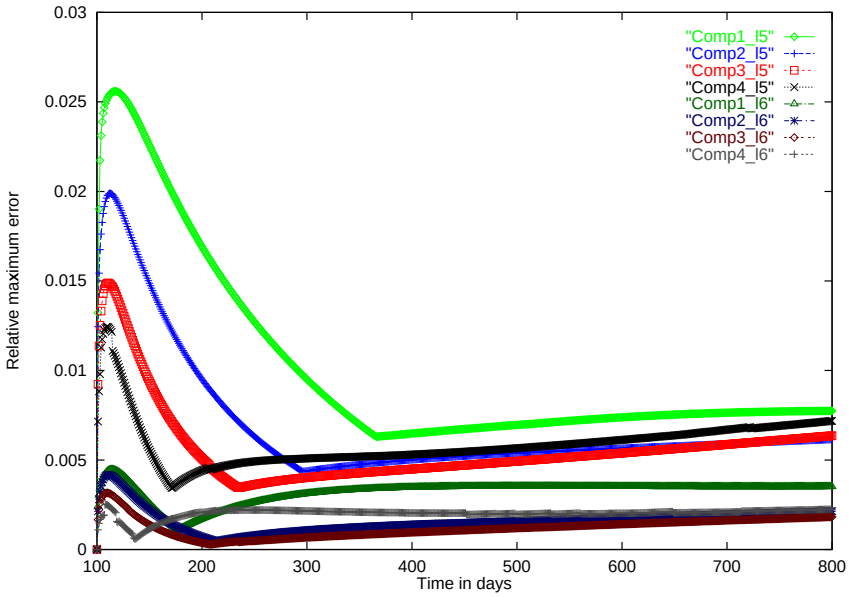

FIG. 4.3. *Comparison of relative maximum error for two successive grid refinements*

Further, we compare the influence of the time discretization on the numerical error. We computed the example on the grid as in the Figure 4.2, but with the time step $\tau = 0.5$ days. The error for both numerical solutions can be compared in the Figure 4.4.

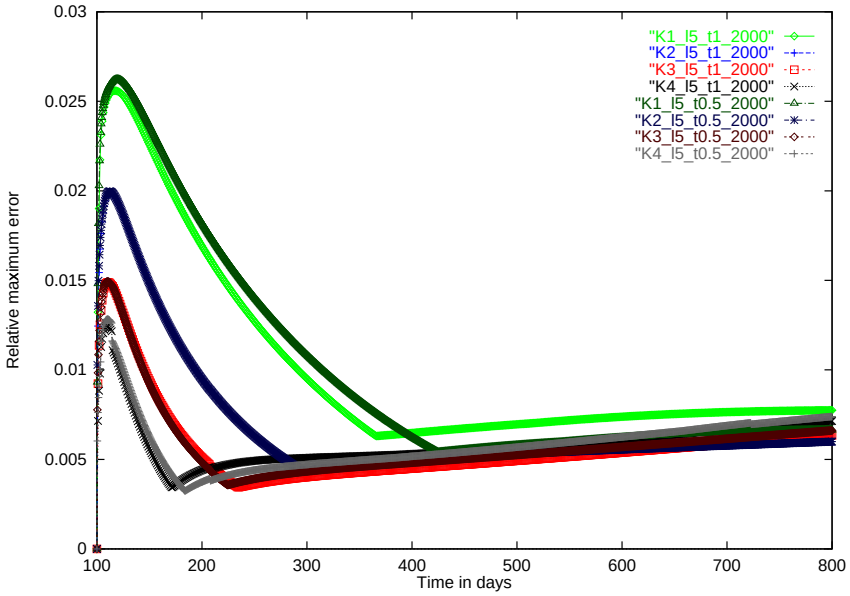

FIG. 4.4. *Comparison of the relative maximum error for two successive time step refinements*

It is clear that a further refinement of the time step gives only marginal reduction of the numerical error. In fact at the initial time period the error is greater with the finer time step (!), compare especially the top lines for C_L^1 and the bottom lines for C_L^4. Nevertheless, after some initial period for the finer time step the error is getting smaller for each component of the numerical solution.

As the analytical solution is well defined only for unbounded domain it is important to insure that the bounded computational domain is large enough to have no undesired influence from the boundary conditions. To illustrate an importamce of this topic we compare the relative maximum error of the numerical solution on the original domain with the solution computed on a smaller domain with the left bottom corner $(-200, -100)$ and the right top corner $(1000, 100)$.

The computations were performed on a coarser grid consisting of 4 096 elements and for a coarser time step $\tau = 10$ days. The numerical results are identical for $t < 1000$ days, but afterwards the error for the last component of the numerical solution starts to grow and similarly for other components later.

It is interesting to note that such undesired influence of the boundary conditions is not "visible" on the numerical solution itself, see the Figure 4.6. There the numerical solution at $t = 1300$ days for C_L^3 and C_L^4 should be already "corrupted", but it can be seen only hardly from the pictures.

Finally, to demonstrate a capability of the developed package RNT we present an analogous, but more complex test example with 9 components for the system (2.2), (2.5), (2.6) and (2.9), see the Figure 4.7 for an illustration of numerical results.

In this Figure a row of 4 pictures shows the contour lines of a particular radionu-

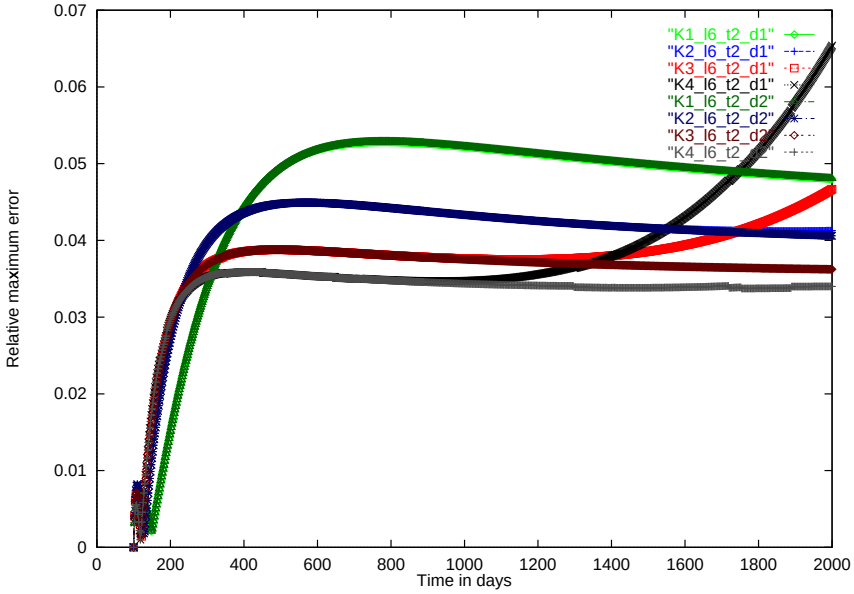

FIG. 4.5. *The error of the numerical solution on the larger and smaller domain*

FIG. 4.6. *Numerical solutions for* C_L^3 *and* C_L^4 *at* $t = 1300$ *days on the smaller domain*

clide concentration in the mobile and the immobile groundwater and the corresponding adsorbed concentrations. The pictures in a single column represents a decay chain. Both nuclides Th-234 and Am-242 in the 4th row decays to the nuclide U-234 in the fifth row.

The computational grid consisted of 4 096 elements with 36 discrete unknowns per each vertex of the grid. The example was computed on a Power Macintosh G3 for 1 300 time steps and the computations took about 16 hours.

5. Conclusions. In this paper the mathematical model was presented that enhances the standard model of the transport of radionuclides decay chain in the flowing groundwater by considering the exchange processes with the immobile pore groundwater and the sorption kinetic processes. The code validation was performed that confirmed for particular examples the capability of the software package to solve well numerically the analytical model.

REFERENCES

[1] P. Bastian, K. Birken, K. Eckstein, K. Johannsen, S. Lang, N. Neuss, and H. Rentz-Reichert. UG - a flexible software toolbox for solving partial differential equations. *Computing and Visualization in Science*, 1(1):27–40, 1997.

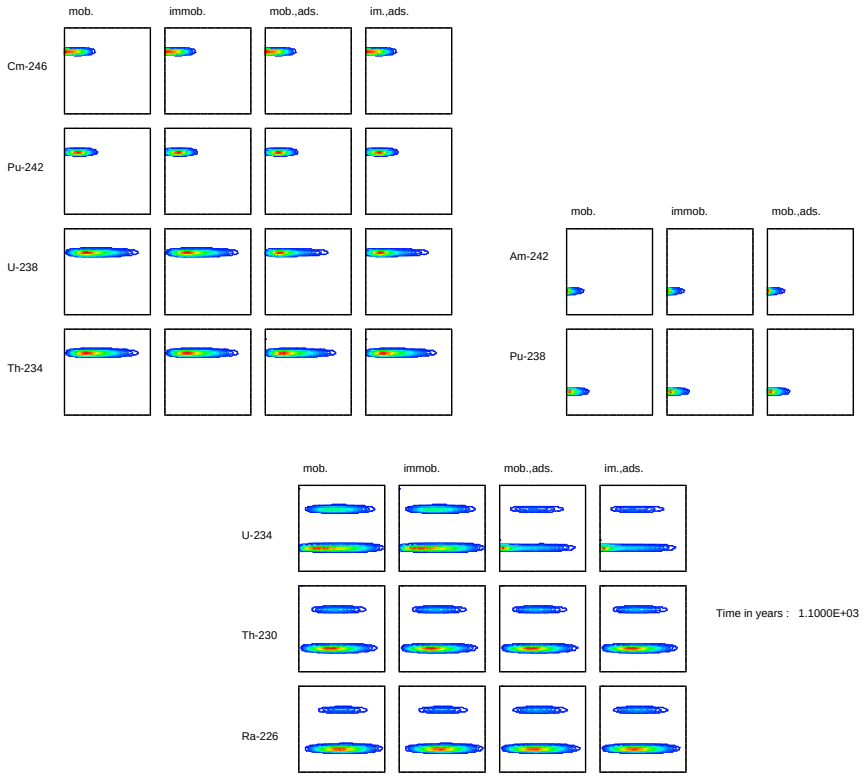

FIG. 4.7. *An illustration of numerical solution for the complex test example*

[2] P. Bauer, S. Attinger, and W. Kinzelbach. Transport of a decay chain in homogenous porous media: Analytical solutions. *Journal of Contaminated Hydrology*, submitted.
[3] J. Bear. *Dynamics of Fluids in Porous Media*. Dover Publication, Inc., New York, 1988.
[4] Z. Cai. On the finite volume element method. *Numer. Math.*, 58:713–735, 1991.
[5] E. Fein, T. Kühle, and U. Noseck. Entwicklung eines Programms zur dreidimensionalen Modellierung des Schadstofftransportes. Fachliches Feinkonzept, Braunschweig, 2000.
[6] P. Frolkovič and H. De Schepper. Numerical modelling of convection dominated transport coupled with density driven flow in porous media. *Advances in Water Resources*, to appear.
[7] W. Kinzelbach. *Numerische Methoden zur Modellierung des Transport von Schadstoffen in Grundwasser*. Schriftenreihe Wasser-Abwasser, Oldenburg, 1992.
[8] N. Neuss. A new sparse matrix storage methods for adaptive solving of large systems of reaction-diffusion-transport equations. In Keil et. al., editor, *Scientific computing in chemical Engineering II*, pages 175–182. Springer-Verlag Berlin-Heidelberg-New York, 1999.
[9] D. Ouazar, A.H.-D. Cheng, and A.D. Kizamou. An object oriented pumping test expert system. *Journal of Computing in Civil Engineering*, 10(1):4–9, 1996.
[10] S. V. Patankar. *Numerical heat transfer and fluid flow*. Hemisphere Publishing Corporation, 1980.